

# Microstrip Dual-Band Bandpass Filter Using U-Shaped Resonators

Eugene A. Ogbodo<sup>1, \*</sup>, Yi Wang<sup>1</sup>, and Kenneth S. K. Yeo<sup>2</sup>

**Abstract**—Coupled resonators are widely used in the design of filters with dual-passband responses. In this paper, we present a dual-band bandpass filter using only couplings between adjacent resonators without cross-couplings. The dual-band bandpass filter with centre frequencies of 1747 MHz and 1879 MHz respectively is designed and fabricated using microstrip U-shaped resonators. Using the coupled resonator pair as a dual-band cluster, a miniaturised structure is achieved as compared to the conventional topology. The measured responses agree closely with the simulations.

## 1. INTRODUCTION

As the modern microwave communication equipment develops, there is a need for lighter and more efficient devices, which has led to the design of dual-band and multiband components, such as antennas, amplifiers, and filters. With the growing interest in the design of dual-band bandpass filter (BPF), many authors [1–5] have used different circuit models and microstrip geometries to achieve the dual-band BPFs. Two parallel filters were connected to actualise a dual-band BPF [5]. By inserting a stop-band into a wide-band, a dual-band filter was achieved [6]. Although [5] and [6] provided the desired responses, they lacked the flexibility to reduce the sizes of the structures. [7] employed stepped impedance resonators (SIRs) in the design of dual-band BPF. [8] used a dual-mode square patch resonator.

In this paper, a coupled U-shaped resonator pair is used to generate the two required pass band frequencies. Three such resonator pairs are then coupled together to form the dual-band BPF. Compared with [7] and [8], it is easier to adjust the positions of the two bands using the proposed structure. A synthesis method similar to [1] has been used to extract the coupling coefficients. However, in contrast to the design in [1] this filter has no DC path and has better out-of-band rejection performance below the lower passband down to DC.

## 2. FILTER DESIGN

A microstrip dual-band BPF has been proposed and designed to have the following specifications:

- Center frequency of the lower and upper passbands,  $f_{0,BPL}$  and  $f_{0,BPU}$ : 1747 MHz and 1879 MHz.
- Passband return loss: 20 dB.
- Fractional bandwidth of lower and upper passband,  $BW_L$  and  $BW_U$ : 4.3%.

A sixth-order Chebyshev dual-band BPF was designed to have a ripple factor of 0.043 dB. The design started with a normalised third-order low-pass prototype filter (LPF) [9] as shown in Fig. 1. The normalised LPF was then made to consist of only shunt reactive components by introducing admittance

---

*Received 23 July 2015, Accepted 3 February 2016, Scheduled 16 February 2016*

\* Corresponding author: Eugene A. Ogbodo (e.a.ogbodo@gre.ac.uk).

<sup>1</sup> Electrical, Electronic and Computer Engineering, University of Greenwich, Medway Campus, Kent, U.K. <sup>2</sup> School of Architecture, Computing and Engineering, University of East London, London, U.K..

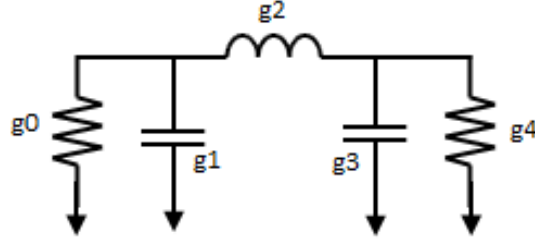


**Figure 1.** Normalised low pass prototype filter;  $g_0 = g_4 = 1$ ,  $g_1 = g_3 = 0.8515$  and  $g_2 = 1.1031$ .

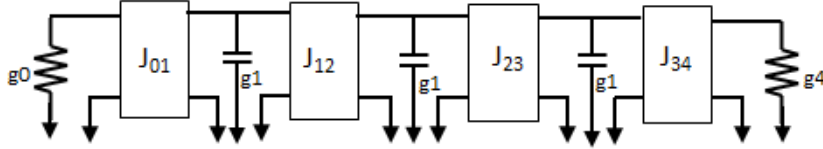


**Figure 2.** Normalised low pass filter with only shunt reactive components;  $J_{01} = J_{34} = 1$  and  $J_{12} = J_{23} = 0.879$ .

inverters ( $J$ -inverter) into the circuit [10]. At this stage, all the low-pass filter parameters are equal to  $g_1$  as shown in Fig. 2. The values of the  $J$ -inverters can be achieved using Eq. (1).

$$J_{01} = J_{n,n+1} = 1 \quad (1a)$$

where  $n$  is the order of the low pass filter. In this work,  $n = 3$ . For  $1 \leq m < n$ ,

$$J_{m,m+1} = \sqrt{\frac{g_1^2}{g_m g_{m+1}}} \quad (1b)$$

A further frequency transformation was carried out on the circuit by transforming the shunt reactive component (capacitor) into a dual-band BPF component. Each capacitor in the circuit was transformed into two shunt  $LC$  resonators, one of a series type and the other of a parallel type [1] as displayed in Fig. 3. The new parameter values can be obtained using Eq. (2).

$$L_a = \frac{\text{FBW}_0 Z_0}{g_1 \omega_c (\omega_2 - \omega_1)} \quad (2a)$$

$$C_a = \frac{1}{L_a \omega_0^2} \quad (2b)$$

$$L'_1 = \frac{\text{FBW}_0 (\omega_2 - \omega_1) Z_0}{g_1 \omega_c \omega_0^2} \quad (2c)$$

$$C'_1 = \frac{1}{L'_1 \omega_0^2} \quad (2d)$$

where  $\omega_c = 1$  rad/s (the cut-off angular frequency of the prototype low-pass filter),  $\omega_0$  is the centre angular frequency  $\omega_0 = \sqrt{\omega_1 \omega_2}$ ,  $\omega_1$  the centre angular frequency of the first passband,  $\omega_2$  the centre angular frequency of the second passband,  $\text{FBW}_1$  the fractional bandwidth for each of the pass bands, and  $\text{FBW}_0$  is defined as

$$\text{FBW}_0 = \text{FBW}_1 \frac{\omega_2 + \omega_1}{\omega_2 - \omega_1} = 1.174 \quad (2e)$$

To achieve the impedance scaling [8], the  $J$ -inverters were scaled using Eq. (3) where  $Z_0$  is the system impedance of  $50 \Omega$ . Fig. 4 shows the dual-band BPF circuit with the scaled impedance.

$$J'_{m,m+1} = \frac{J_{m,m+1}}{Z_0} \quad (3)$$

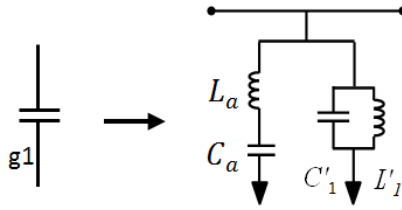


Figure 3. Low-pass to dual-band bandpass transformation.

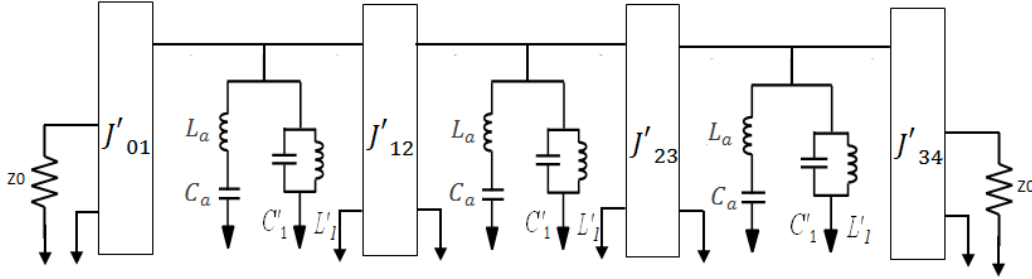


Figure 4. Dual-band BPF with shunt LC resonators;  $J'_{01} = J'_{34} = 0.02 \text{ S}$ ,  $J'_{12} = J'_{23} = 0.018 \text{ S}$ ,  $L_a = 82.659 \text{ nH}$ ,  $C_a = 0.093 \text{ pF}$ ,  $L'_1 = 0.441 \text{ nH}$  and  $C'_1 = 17.393 \text{ pF}$ .

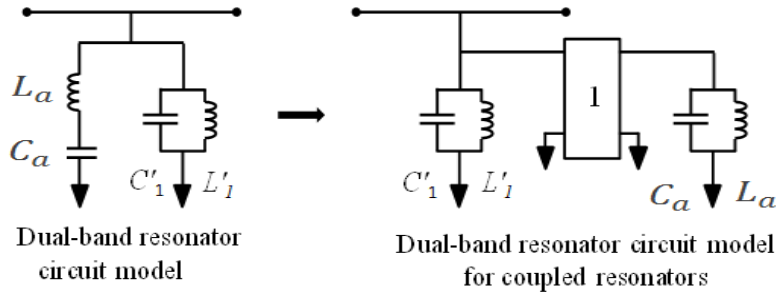


Figure 5. Dual-band resonator circuit model.

In order to achieve a dual-band bandpass filter circuit model with coupled resonators, the mixed series-parallel dual-resonator circuit is transformed into two resonators of the same type (parallel type) coupled through a unity  $J$ -inverter ( $J = 1 \text{ S}$ ) [1]. The transformation pattern used is shown in Fig. 5 whereas the final circuit model is shown in Fig. 6(a). Fig. 6(b) illustrates the coupling path of the dual-band BPF. It is clearly shown that there is no cross-coupling path in this topology. Without cross-coupling, the filter can be easily achieved using simple folded half-wavelength resonators. The calculated response from the circuit model of the dual-band BPF is presented with solid lines in Fig. 6(c). From the circuit model, the coupling coefficients of the dual-band filter can be determined using Eqs. (4) and (5) and the external quality factor  $Q_{ex}$  using Eq. (6) [3].

$$M_{1,1'} = M_{2,2'} = M_{3,3'} = J \sqrt{\frac{L'_1 L_a}{C'_1 C_a}} = 0.073 \quad (4)$$

$$M_{1,2} = M_{2,3} = J'_{12} \sqrt{\frac{L'_1}{C'_1}} = 0.089 \quad (5)$$

$$Q_{ex} = \frac{\omega_0 C'_1}{J'_{01}} = 9.9 \quad (6)$$

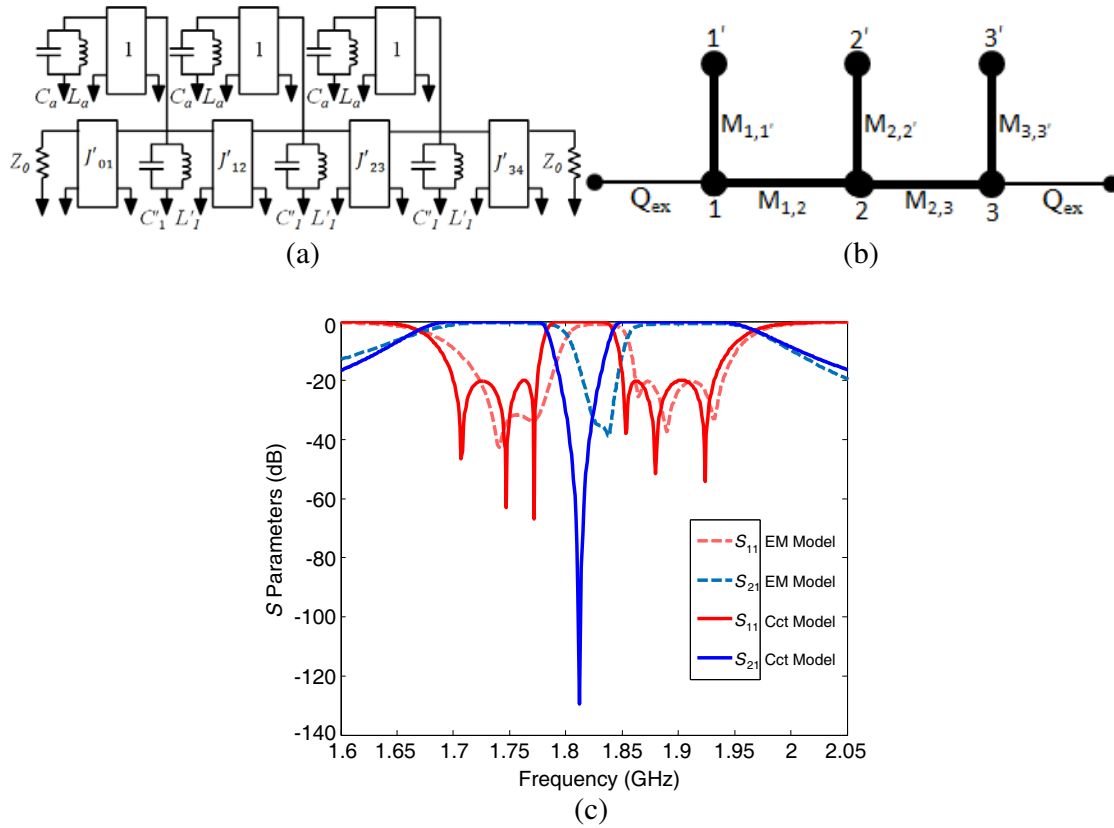


**Figure 6.** (a) Equivalent circuit model;  $L'_1 = 0.441$  nH,  $C'_1 = 17.393$  pF,  $C_a = 82.659$  nF,  $L_a = 0.093$  pH, (b) dual-band coupling path, and (c) the calculated responses from the circuit model and the simulated responses from the EM model.

### 3. MICROSTRIP IMPLEMENTATION

Here the U-shaped microstrip resonators [11, 12] were used in a parallel configuration. Using Agilent ADS EM simulator, full-wave electromagnetic (EM) simulations were performed to extract the coupling coefficients, as well as the external quality factor. With the arrangements of two U-shaped resonators

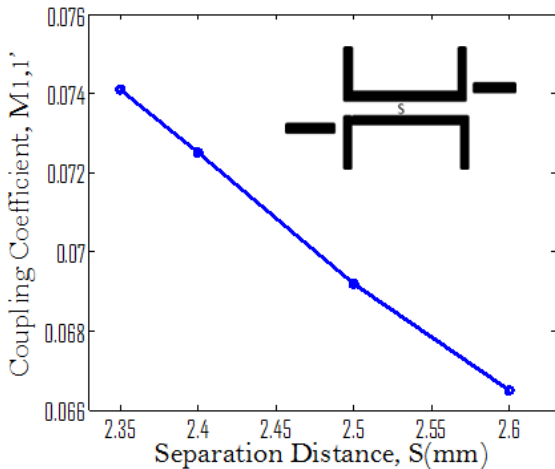


**Figure 7.** Coupling of  $M_{1,1'}$  against spacing ( $S$ ).

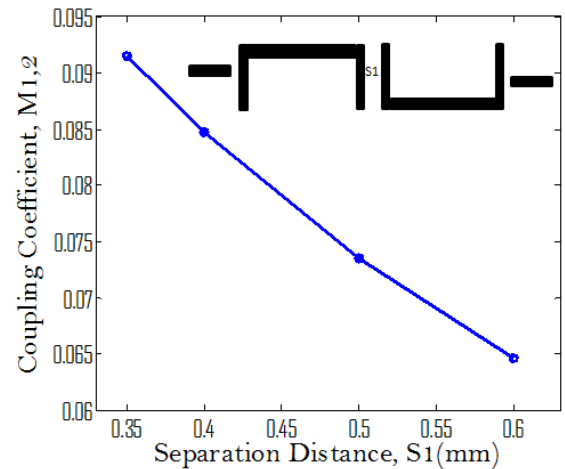


**Figure 8.** Coupling of  $M_{1,2}$  against spacing ( $S_1$ ).

as shown in Fig. 7, the coupled resonators resemble one dual-mode ‘cluster’ resonator which can be considered as a dual-band resonator. The coupling coefficients of  $M_{1,1'}$ ,  $M_{2,2'}$  and  $M_{3,3'}$  were extracted by varying the spacing ( $S$ ) between the two U-shaped resonators. A graph of the coupling coefficient against  $S$  was plotted. To determine the coupling coefficients of  $M_{1,2}$  and  $M_{2,3}$ , the configuration in Fig. 8 was simulated. The coupling coefficient against the spacing  $S_1$  is also illustrated.

In order to obtain the external quality factor at the input and output (I/O), an arrangement was set up as shown in Fig. 9. At Port-1, a 50 Ohm feeder line is tapped to the first resonator whereas Port-2 is weakly coupled to the resonator to remove the external coupling at Port-2. The tapping point of the feeder line as defined by  $Y$  on the resonator was adjusted. The length  $X$  of the resonator was reduced; this is to compensate the loading effect from the tapped feeder.

After extracting and satisfying the parameters needed for the design of the dual-band bandpass filter, the entire layout was put together as shown in Fig. 10. After optimisation, the simulated responses of the EM model were presented using dashed lines as shown in Fig. 6(c).

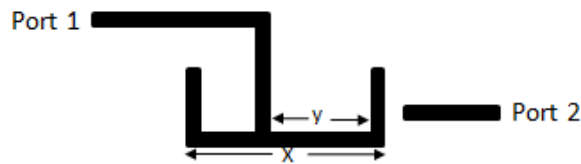


Figure 9. Resonator arrangement for extracting  $Q_{ex}$ .

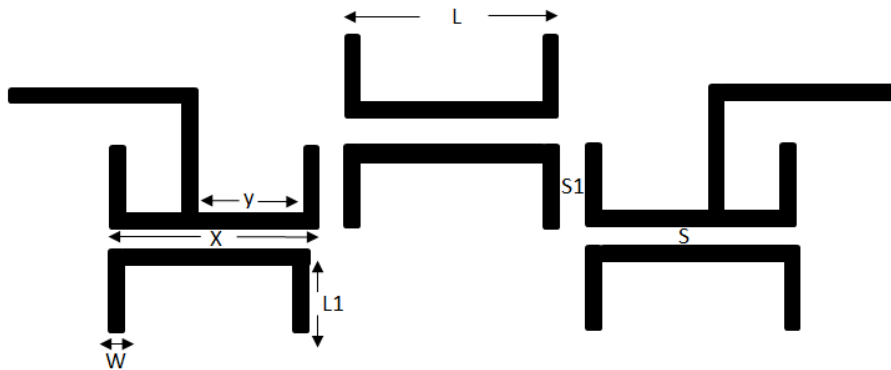


Figure 10. Dual-band microstrip filter layout.  $L = 17.2$  mm,  $L_1 = 6.8$  mm,  $W = 1.126$  mm,  $X = 17$  mm,  $S = 2.4$  mm,  $S_1 = 0.35$  mm,  $Y = 12$  mm.

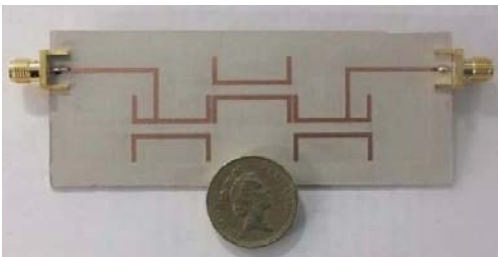


Figure 11. Fabricated microstrip dual-band filter.

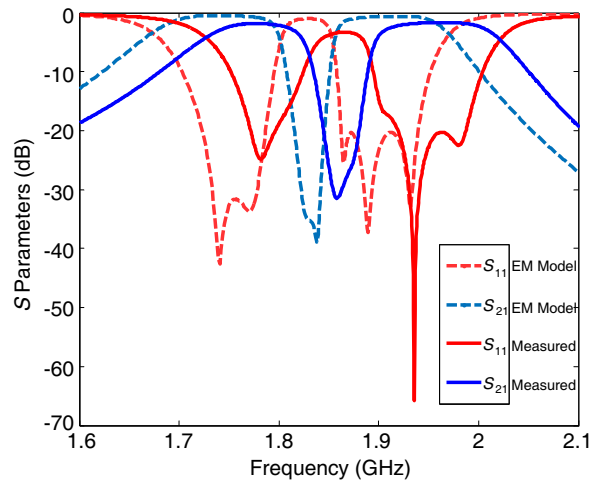


Figure 12. Simulated and measured responses.

#### 4. FABRICATION AND MEASUREMENTS

RT/Duroid 6010LM substrate from Rogers® was used for the fabrication. The dielectric constant of the material is 10.2 with a loss tangent of 0.0035 and a thickness of 1.27 mm. Fig. 11 shows the fabricated prototype. The microstrip dual-band filter was fabricated using Protomat C60 micro-milling process. Agilent E5062A Network Analyser was used to measure the filter. A comparison of the simulated and measured response is shown in Fig. 12. It can be seen that a reasonably good agreement is achieved at both passbands with a return loss close to 20 dB. Due to the machining tolerance, the measured responses can be seen shifted to the higher frequency by 40 MHz. The minimum measured insertion loss in the passband is less than 2 dB.

#### 5. CONCLUSION

In this paper, a dual-band BPF were proposed to have 1747 MHz and 1879 MHz for its low and high passband respectively. A pair of coupled U-shaped resonators behaving as a dual-band resonator cluster was arranged to resonate at the centre frequencies of the two passbands. Three pairs of the clusters were then coupled to each other in a parallel configuration. With this type of configuration, the realization of the dual bands can be achieved without resorting to any cross couplings. This design also has the flexibility to control the position of the two bands.

#### REFERENCES

1. Guan, X., Z. Ma, P. Cai, Y. Kobayashi, T. Anada, and G. Hagiwara, "Synthesis of dual-band filters using successive frequency transformations and circuit conversions," *IEEE Microwave and Wireless Component Letters*, Vol. 16, No. 3, 110–112, 2006.
2. Yeo, K. S. K. and M. J. Lancaster, "8 pole high temperature superconductor microstrip dual band bandpass filter design," *IEEE MTT-SIMS Digest*, 1–4, 2011.
3. Yeo, K. S. K., M. J. Lancaster, and J.-S. Hong, "The design of microstrip six-pole quasi-elliptic filter with linear phase response using extracted-pole technique," *IEEE Trans. Microw. Theory Tech.*, Vol. 49, No. 2, 321–327, 2002.
4. Zhao, L.-P., D. Li, Z.-X. Chen, and C.-H. Liang, "Novel design of dual-mode dual-band bandpass filter with triangular resonators," *Progress In Electronics Research*, Vol. 77, 417–424, 2007.
5. Miyake, H., S. Kitazawa, T. Yamada, and Y. Nagatomi, "A miniaturised monolithic dual band filter using ceramic lamination technique for dual mode portable telephones," *IEEE MTT-S Int. Dig.*, 789–792, 1997.
6. Tsai, L. C. and C. W. Hsue, "Dual-band bandpass filters using equal-length coupled serial-shunted lines and Z-transform technique," *IEEE Trans. Microw. Theory Tech.*, Vol. 52, No. 4, 1111–1117, Apr. 2004.
7. Chang, S. F., Y. H. Jeng, and J. L. Chen, "Dual-band step-impedance bandpass filter for multimode wireless LANs," *Electron. Lett.*, Vol. 40, 38–39, Jan. 2004.
8. Yeo, K. S. K. and A. O. Nwajana, "A novel microstrip dual-band bandpass filter using dual-mode square patch resonators," *Progress In Electromagnetics Research C*, Vol. 36, 233–247, 2013.
9. Matthaei, G., L. Young, and E. M. T. Jones, *Microwave Filters, Impedance-matching Networks, and Coupling Structures*, Artech Houston, Boston, 1980.
10. Cohn, S. B., "Direct-coupled-resonator filters," *Proceedings of the IRE*, Vol. 45, No. 2, 187–196, 1957.
11. Pozar, D. M., *Microwave Engineering*, 3rd Edition, Wiley, New York, 2005.
12. Hong, J. S., *Microstrip Filters for RF/Microwave Applications*, John Wiley & Sons, Inc., New Jersey, 2011.